



Development of nanocomplex mimic-hsa-miR-143-3p loaded exosome (exo-miR) to inhibit viability, migration and proliferation of triple-negative breast cancer

Fita Nilasari¹, Sofia Mubarika Haryana^{2,*}, Dwi Aris Agung Nugrahaningsih³, Pamungkas Bagus Satriyo³

¹Study Program of Master in Biotechnology, Graduate School, Universitas Gadjah Mada, Yogyakarta 55281, Indonesia

²Department of Histology and Cellular Biology, Faculty of Medicine Public Health and Nursing, Universitas Gadjah Mada, Yogyakarta 55281, Indonesia

³Department of Pharmacology and Therapy, Faculty of Medicine Public Health and Nursing, Universitas Gadjah Mada, Yogyakarta 55281, Indonesia

*Corresponding author: rikaharyana@ugm.ac.id

SUBMITTED 4 January 2024 REVISED 28 March 2024 ACCEPTED 1 May 2024

ABSTRACT Breast cancer represents the highest number of cancer cases in Indonesia, with triple-negative breast cancer (TNBC) being a common subtype (10–15%). MicroRNAs play a role in cancer epigenetics and contributing as core factors to the disease. The expression of miR-143-3p have been found to be lower in breast cancer samples from Yogyakarta and Central Java. It is known that miR-143-3p functions as a tumor suppressor in breast cancer, and its overexpression corresponds with an increased survival rate. The structure of miRNA is quickly degraded, an enhanced delivery system for miRNA is required. Exosomes are indeed emerging as natural delivery agent. A new approach represents that exosomes will be transfected with mimic-hsa-miR-143-3p yield an exo-miR. The research aimed to examine how exo-miR affects viability, migration, and proliferation using 4T1 cell line. The Exo-Fect-based method was used to transfect mimic-hsa-miR-143-3p into exosomes. The MTT assay, wound healing assay, and colony formation assay were used as functional assay. The MTT assay revealed that 7.5 μ L/ 250,000 particles exo-miR obtained a lower percentage of cell viability (58%) than the control (99.7%). The wound healing assay showed that transfection of 37.5 μ L/ 1,250,000 particles exo-miR was able to suppress migration by the percentage of wound closure (67%) compared to the control (100%). Exo-miR also had a significant ($p < 0.001$) effect on colony-forming abilities, as shown by fewer colonies (32) compared to the control (132). This findings demonstrated that exo-miR represents a promising targeted approach in cancer therapy.

KEYWORDS Exosome; Migration; mimic-hsa-miR-143-3p; Proliferation; TNBC; Viability

1. Introduction

Breast cancer is the leading cause of death for women worldwide, and Indonesia has the highest number of patients. According to the statistic number from the World Health Organization (WHO) in *Global Cancer Observatory* (2020), the percentage of breast cancer patients in Indonesia reaches 16.6% or 65,858 patients out of all cancer patients. The triple-negative breast cancer (TNBC) subtype is the most common type of breast cancer (10–15%) and the cause of high patient mortality rates (Mehanna et al. 2019). TNBC is an aggressive type of breast cancer that has the worst prognosis compared to other subtypes (Hermansyah et al. 2021). TNBC which lacks estrogen receptors (ER), progesterone receptors (PR), and human epidermal growth factor receptor-2 (HER-2) are highly invasive and rapidly metastasizes (Rayson et al. 2018). Most cases of TNBC had a high degree of seriousness, fast an-

giogenesis, lymphatic invasion, and increased tumor infiltrating lymphocyte (TIL) levels might produce a worse prognosis than other subtypes (Radosa et al. 2017).

Long noncoding RNAs (lncRNAs) and small noncoding RNAs (sncRNAs) are epigenetic regulators that play a role in intracellular and intercellular signaling in cancer. MicroRNA (miRNA) is a specific subtype of sncRNA that able to post-transcriptionally regulate several target genes via specific targets on the 3' UTR mRNA (Klinge 2018). MiRNAs have an ability to regulate cancer cells at the molecular level that led to their widespread use as biomarkers and novel therapies.

Previous study successfully analyzed miRNAs from tumor tissue of TNBC patients in the Yogyakarta and Central Java region (Satriyo et al. 2020). The nanostring analysis revealed a significant dysregulation of miR-143-3p related to cancer cell progression. High expression of miR-

143-3p was associated with a good prognosis and survival rate. This finding showed that treatment using miRNA-based therapy have opened a new promising perspective but also has a several challenges. miRNA requires a delivery system that can work specifically and has a stable structural arrangement when delivering molecules to cellular systems (Dasgupta and Chatterjee 2021).

Exosomes are a potential target for delivering molecules. Exosomes are extracellular vesicles that range in size from 30-150 nm (Bhome et al. 2018). Exosomes can be easily isolated from any body fluid. Exosomes are not immunogenic and regulated for delivering molecules to target cells (Samanta et al. 2018), can actively or passively carry compounds to cancer cells such as drug molecules, nucleic acids, and proteins. Exosomes are more stable than lipid nanoparticles because macrophages and the reticuloendothelial system may remove lipid nanoparticles. Exosomes generated by cells are also highly biocompatible, resulting in minimal toxicity and immunogenicity (Kim et al. 2021).

Exogenous miRNA-based gene therapy approaches include by exosomes are a novel treatment option for cancer. Anti-miRNA oligonucleotides (AMO) and miRNA mimics (miR mimic) are a few examples of exogenous miRNAs that can be applied. The miR mimics are used for enhanced inhibition in cancer cells (tumor suppressor), whereas AMO is used to inhibit tumor-promoting miRNA (oncomiR). The mimic-hsa-miR-143-3p is a hsa-miR-143-3p synthetic miRNA. According to research data, miR-143-3p functions as a tumor suppressor in the development and carcinogenesis of breast cancer (Xia et al. 2018). Transfection exogenous miRNA mimics (mimic-hsa-miR-143-3p) into exosomes (exo-miR) can influence pathophysiological changes in breast cancer cells. High expression of miR-143-3p in cancer cells, reducing viability and suppressing proliferation (Zhang et al. 2016).

This study determined the potential of mimic-hsa-miR-143-3p encapsulated exosome (exo-miR) on 4T1 cell line. The transfection method was performed according to the protocol of Exo-Fect™ Exosome Transfection Kit (cat. EXFT20A-1, System Biosciences). We demonstrated the effects of exo-miR on 4T1 cell line using MTT assay, scratch wound healing assay, and colony formation assay as a functional assay. This study presents a significance result of a newly complex exosome-mimic miR (exo-miR) in having a potential to inhibit viability, migration, and proliferation of breast cancer *in vitro*.

2. Materials and Methods

2.1. Exosome isolation and characterization

Exosomes were isolated from secretomes of mesenchymal stem cells (MSC), product of Tristem Medika Indonesia company. The exosomes characterization resulted quantitative data in the form of particles (per millilitre) (/mL). Exosome samples were found to contain 2.4×10^8 particles/mL. The average size of exosome samples is 117 nm

(Agung Nugrahaningsih et al. 2023). In accordance with the the framework, exosome nanoparticles range in size is from 30 to 150 nm (Vestad et al. 2017).

2.2. Cell culture

Handling procedure for the 4T1 cell line was the one according to the protocol from American Type Culture Collection (<https://www.atcc.org/>). The 4T1 cell line were cultured in DMEM medium (Gibco™ 11965092) with 10% fetal bovine serum (FBS) (Gibco™ 16000044) supplementation, 1% penicillin-streptomycin (Gibco™ 15140122) and 0.5% amphotericin-B (Gibco™ 15290018). The vial was thawed in a 37 °C water bath about 2 min, followed by transferring the vial contents (cells) into the conical centrifuge tube containing 5 mL complete medium, then the tube was centrifuged at 2,000 rpm for 5 min. The supernatant was then removed, and the cell pellet was resuspended using 1 mL complete medium. The cells (1 mL) were transferred into a culture dish (100 mm) (iwaki 3020-100) containing 9 mL complete medium and were gently homogenized. The cell culture was incubated in a humidified incubator (37 °C, CO₂ 5%). When the cells were 70–80% confluent, the cells were then sub-cultured. The medium was removed, the cells were washed with 2 mL of phosphate-buffered saline (PBS) (Gibco™ 10010023), and slowly homogenized. After dispensing the PBS, the cells were treated with 1 mL of 0.25% Trypsin-EDTA (Gibco™ 25200056) as a detaching agent and then incubated for 3 min in the incubator (37 °C, CO₂ 5%). Cells were added with 4 mL of complete DMEM and homogenized. The cells were transferred to the conical tube and centrifuged for 5 min at 2,000 rpm. After dispensing the supernatant and resuspending the pellet with 1 mL of complete medium, the cells were count using the Trypan Blue method. Amount of 300,000 cells/100 µL were transferred to a culture dish (100 mm) (iwaki 3020-100) and slowly homogenized until the cells were evenly distributed. The cells were incubated at 37°C, CO₂ 5% about 48–72 hour (h) and then repeatedly sub-cultured.

2.3. Transfection mimic-hsa-miR-143-3p into exosomes

Synthetic miR (mimic-hsa-miR-143-3p) custom from Integrated DNA Technologies (IDT) was transfected into exosomes according to the protocol of Exo-Fect™ Exosome Transfection Kit (cat. EXFT20A-1, System Biosciences). The following components were added to a 1.5 mL microtube: 10 µL Exo-Fect solution, 2 µL mimic-hsa-miR-143-3p (20 pmol) dissolved in 19.8 µL Nuclease Free Water (NFW), 70 µL sterile PBS, 41.7 µL exosomes (107 exosome particles) dissolved in PBS 8.3 µL sterile. The components were combined to yield a total volume of 150 µL. The samples were homogenized by inverting them three times, without vortexing. The samples were incubated in a 37 °C water bath with a treatment shaker speed of 150 rpm for 10 min. Samples were immediately transferred to an ice box and incubated for 10 min. The

volume of 30 μL of ExoQuick-TC reagent was added into the sample. The sample was homogenized by inverting 6 times without vortexing. Sample was incubated in ice box or at 4 $^{\circ}\text{C}$ for 30 min. Samples were centrifuged at 14,000 rpm for 3 min. After dispensing the supernatant, the pellet was resuspended in 300 μL of sterile PBS. The exo-miR solution can directly transfected into the cell or can be stored at -20 $^{\circ}\text{C}$.

2.4. Transfection confirmation test using siRNA labelled Texas-Red

The sterile coverslips (cat no. 1101-018, Cosmo Bioscience Inc.) were added to the centre of the 6-well plate (iwaki 3810-006N). The DMEM (3 mL/well) was added. The 4T1 cell line was cultured at a cell count of 100,000 cells/well. Cells were incubated for 24 h at 37 $^{\circ}\text{C}$ (5% CO_2). Confirmation of transfection was performed using siRNA labelled with Texas-Red, according to the protocol of Exo-Fect™ Exosome Transfection Kit (cat. EXFT20A-1, System Biosciences). Cells were added with complex exosome + siRNA + Texas-Red as much as 150 μL (5,000,000 particles exo-miR), and incubated for 24 h at 37 $^{\circ}\text{C}$ (5% CO_2). To confirm the transfection effectiveness, cells were observed by using a confocal microscope/fluorescent microscope with Standard Red Fluorescent Protein (RFP) filter settings. Transfection is considered effective if the cells emit a red light in accordance with Texas-Red standards.

2.5. MTT assay

Cell viability assay protocol (MTT assay) was conducted based on the previous study with modifications to the number of cells and concentrations (Ysrafil et al. 2020). The 4T1 cell line was cultured in 96-well plates (iwaki 3860-096) at a cell count of 3,935 cells/well using DMEM, then incubated overnight at 37 $^{\circ}\text{C}$ (5% CO_2). Cells were transfected with exo-miR at various concentrations, i.e. (a) 7.5 μL /250,000 particles exo-miR, (b) 3.75 μL /125,000 particles, (c) 1.875 μL /62,500 particles, as well as a control treatment (control 4T1 cell line, control exosome + kit (E*), control mimic-hsa-miR-143-3p, and control exosomes) using volume based on the concentrations using at point (a). Each sample and control were conducted in triplicate and incubated for 24 h (37 $^{\circ}\text{C}$, 5% CO_2). After 24 h, the medium was removed and then added with 100 μL (0.5 mg/mL) MTT (3-[4,5-dimethylthiazol-2-yl]-2,5 diphenyl tetrazolium bromide) solution. The samples were incubated at 37 $^{\circ}\text{C}$, 5% CO_2 for 4 h. To stop the reaction, 100 μL of sodium dodecyl sulfate (SDS) (10% SDS in 0.01 M HCl) was added to the cells. The plates were incubated at room temperature for overnight in the dark. The absorbance was read at 595 nm using microplate reader.

2.6. Wound healing assay

The 4T1 cell line was cultured on 24-well plates (iwaki 3820-024) at a cell count of 200,000 cells/well in DMEM with 0.5% FBS. Cells were incubated at 37 $^{\circ}\text{C}$, 5% CO_2 for 24 h. A gap or cell free area was created by man-

ually scratch using pipette tip (yellow/white tip) vertically (Jonkman et al. 2014). The medium was removed, cells then washed with medium before being transfected with different concentrations of exo-miR, i.e. (a) 37.5 μL /1,250,000 particles exo-miR, (b) 18.75 μL /625,000 particles, (c) 9.375 μL /312,500 particles, as well as a control treatment (control 4T1 cell line, control exosome + kit (E*), control mimic-hsa-miR-143-3p, and control exosomes) using volume based on concentration using at point (a). Each sample and control were tested in triplicate and incubated for 24 h (37 $^{\circ}\text{C}$, 5% CO_2). Cell migration was observed at 0, 12, and 24 h after treatment using OptiLab camera.

2.7. Colony formation assay

The 4T1 cell line was cultured in 6-well plates (iwaki 3810-006N) at a cell count of 100 cells/well in DMEM medium containing 3% FBS. Cells were incubated at 37 $^{\circ}\text{C}$, 5% CO_2 for 24 h. After washing, the cells were transfected with 150 μL exo-miR (5,000,000 particles exo-miR, as mentioned in the Exo-Fect Kit Protocol), as well as control treatment (control exosome + kit (E*), control mimic-hsa-miR-143-3p, and control exosomes). Each sample and control were tested in triplicate and incubated for 10 d at 37 $^{\circ}\text{C}$, 5% CO_2 . Every 72 h, the medium was changed and re-transfected with an exo-miR. Cells were stained with methylene blue 1% in methanol (Pro Analysis grade) after 10 d of incubation. The medium was dispensed and washed with PBS 3 mL/well, PBS was dispensed and then add with methanol 3 mL/well. Incubate the sample in -20 $^{\circ}\text{C}$ about 15 min. The methanol was dispensed and then add with methylene blue (1% in methanol) 3 mL/well. Incubate the sample in room temperature about 3–4 h. Dispense the methylene blue until it is completely clean and then wash gently with PBS once. The data obtained was the number of colonies stained using methylene blue. Images of 6-well plates were then analysed using ImageJ software to count the number of colonies.

2.8. Statistical analysis

Statistical analysis was performed using the Graph Pad Prism by Dotmatics Software (<https://www.graphpad.com>). Numerical data are presented in the form of mean \pm standard deviation (DS). Numerical data were tested for normality using the Shapiro-Wilk test ($\alpha = 0.05$). Comparative analysis of treatment and control using the unpaired t-test. The Pearson's correlation analysis with standard $p < 0.05$, indicated that there were significant differences in the statistical data.

3. Results and Discussion

3.1. Transfection mimic-hsa-miR-143-3p into exosome

Previous research showed that the Exo-Fect method was the most effective when compared to other methods such as electrophoresis, heat shock, saponin and cholesterol-based (de Abreu et al. 2021). The Exo-Fect method can

interact with exosomes via an interaction mechanism on the exosome surface membrane. This surface interaction exposes the exosome's surface membrane, allowing components such as miRNA to enter the lumen via a diffusion process. As a result, exosomes can be simply utilized as carrier agents in gene therapy/targeted therapy. Exo-Fect might improve exosome internalization into the cells.

A siRNA labelled with Texas Red (Texas Red-labelled siRNA) was used in the transfection confirmation test to confirm the availability of Exo-Fect that could transfected mimic-miR into exosome and internalized into the cells. To confirm effective transfection, cells were observed under a confocal microscope/fluorescent microscope with standard RFP filter settings. Transfection was successful when the cells emit a red light in accordance with Texas-Red standards (Figure 1).

The observation using confocal microscope showed that the 4T1 cell line transfected with a positive control in the form of siRNA-labelled Texas Red had a fluorescence intensity of 1.073. The intensity was higher than the negative control, which was 0.182. This fluorescence indicates that the Texas-Red labelled siRNA was successfully transfected into the exosome and can be internalized into the cells. Previous research has revealed that exosomes that introduced into the cells were recognized as a single vesicle, no accumulation at the cells surface, and detected to have cell contact leading to internalization. These findings suggest that exosome uptake is highly efficient. Newly describe showed that exosomes enter the cell by filopodia. Exosome form endosomal trafficking and scanning the endoplasmic reticulum (ER) for potential cargo release (Heusermann et al. 2016). As a result, the exosome-based Exo-Fect method is preferable for regulating cargo internalization.

3.2. Cell viability assay using MTT assay

The exo-miR nanocomplex was further examined for the effect on the 4T1 cell line viability, by using the MTT assay technique. MTT reagent (3-(4,5-dimethylthiazol-2-yl)-2,5-diphenyl-2H-tetrazolium bromide) is a positively charged mono-tetrazolium with four core tetrazole rings

surrounded by three aromatic rings, two phenyl groups, and one thiazolyl ring. MTT reagents can pass cell membranes and mitochondrial membranes of living cells before being reduced to formazan by cell metabolic activity. The reduction of the MTT reagent promotes damage to the core of the tetrazole ring, resulting in the formation of formazan, a water-insoluble violet-blue molecule (Stockert et al. 2018).

The experiment was conducted using a triplicate design to examine the viability of 4T1 cells after the transfection of exo-miR nanocomplexes. The exo-miR concentrations was calculated using the area of the volume provided on the multi-well plate utilized and the number of cells grown in each well. The E* control is an exosome control included with the Exo-Fect kit that does not include miR mimic. The controls are designed to assess the efficacy of mimic-hsa-miR-143-3p on 4T1 cells. The viability of 4T1 cells showed the lowest percentage compared to controls using exo-miR concentrations 7.5 μ L/ 250,000 particles exo-miR (a) (Figure 2). The control used was an E* control (Exosome + Exo Fect), which aimed to determine the functional of mimic-hsa-miR-143-3p on 4T1 cell viability.

The lower percentage in cell viability indicated that there was an inhibitory regulation of 4T1 cell growth caused by the addition of exo-miR. The function of mimic-hsa-miR-143-3p towards inhibition of 4T1 cells can be seen based on the percentage of viability compared to control E* (exosome + kit), mimic-hsa-miR-143-3p, and exosomes (Figure 3). Significant effects on cell viability were observed in 4T1 cells that had been transfected with exo-miR. This data was compared with the controls, including the control E*, exosomes, and mimic-hsa-miR-143-3p, in order to assess the functional effects of the miRNA independently. Concentrations of 7.5 μ L/ 250.000 particles exo-miR (a) was significantly ($p < 0.001$) reduced the viability of 4T1 cells.

The exo-miR nanocomplex is capable of keeping mimic-hsa-miR-143-3p stable, allowing it to be transported to target cells and control inter-cellular signalling. The exosome lipid double layer structure protects the

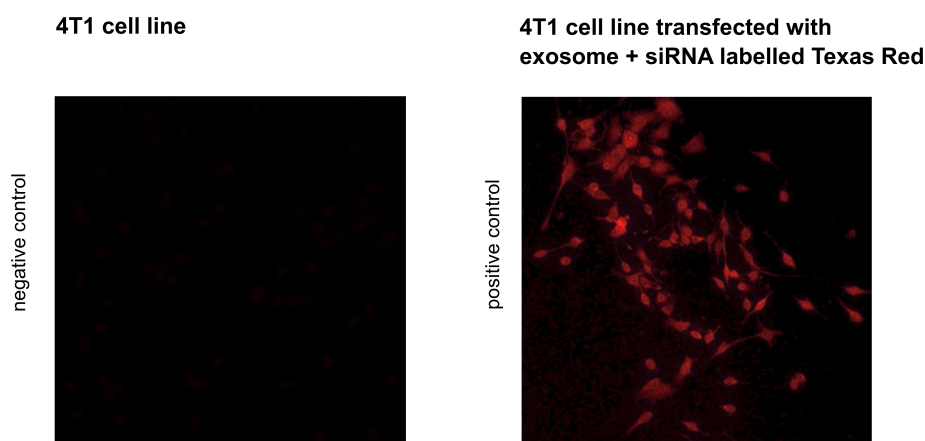


FIGURE 1 4T1 cell line transfected with Texas-Red labelled siRNA to confirm the transfection process.

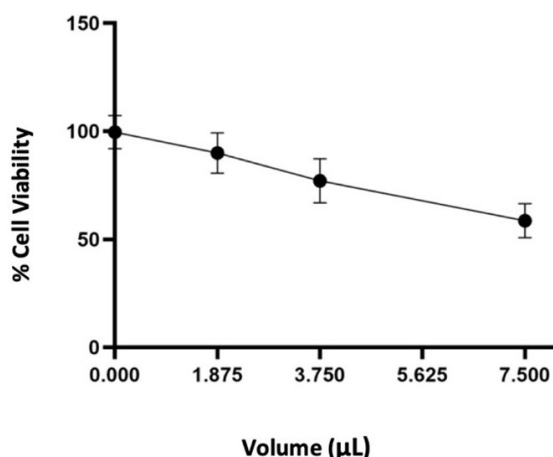


FIGURE 2 Cell viability percentage of 4T1 cells after adding exo-miR nanocomplex with a volume of 1.875 µL (62,500 particles), 3.75 µL (125,000 particles) and 7.5 µL (250,000 particles). The viability of 4T1 cell line was lower than control (E*) (0.000 µL).

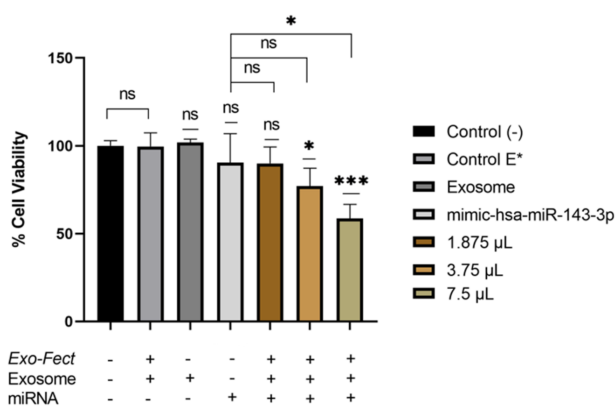


FIGURE 3 MTT assay resulted that cells transfected with exo-miR with a volume of 1.875 µL (62,500 particles), 3.75 µL (125,000 particles) and 7.5 µL (250,000 particles) showed lower viability (58.6%) compared to control (99.7%). ns = not significant; * = $p < 0.05$; *** = $p < 0.001$.

mimic-hsa-miR-143-3p from degradation (Guo et al. 2021). Exosomes are particularly effective delivery vehicles when compared to other synthetic cargo. Through filopodia, the exosome enters the target cell, travels through the endosomal pathway to the endoplasmic reticulum, and ultimately releases miRNA into the cytosol. miRNA will be induced by RNA-induced silencing complex (RISC). The target mRNA will bind to RISC, which allows the target mRNA to degrade in the rough endoplasmic reticulum (Heusermann et al. 2016).

The results of the unpaired t-test on cells transfected with mimic-hsa-miR-143-3p and exosome showed insignificant results ($P > 0.05$) when compared to controls. These data indicated that treatment using mimic-hsa-miR-143-3p and exosome had lower significant effect on 4T1 cell viability. The structure of mimic-hsa-miR-143-3p which is unstable in the circulation system can be degraded by RNase (Lu et al. 2023) so it has lower effect on 4T1 cells.

The exosome control showed an increase in cell via-

bility compared to the control. This increase in cell viability is caused by components in exosomes that can support cancer progression such as proteins, endogenous miRNAs, lipids and several growth factors. Previous research demonstrated that exosomes isolated from MSCs could increase the viability of MCF7 cells because they contain several tumour supporting components (Vallabhaneni et al. 2014). Other studies also support these results that exosomes from MSCs can induce cell viability through the hippo signalling pathway which has implications for tumour progression. Hippo signalling pathway plays a role in the regulation of tumorigenesis (Wang et al. 2016).

3.3. Migration assay using wound healing assay

Cell migration is one of the processes that cancer cells go through on their way to metastasis. Changes in the regulation of cytoskeleton dynamics and focal adhesion, which are connected to cell migratory signals, are involved in the mechanism. Wound healing assay is a common *in vitro* approach for determining cell migration activity in two dimensions. To create a cell-free space, monolayer cells were treated with physical exclusion. The area without cells will induce cells to migrate to the gap area formed.

The wound closure was observed at 0, 12, and 24 h. The areas were examined with an inverted microscope combined to the OptiLab (Miconos) device. ImageJ software (<https://fiji.sc/>) was used to analyse the results of observations in the form of pictures to determine the area closure at each hour of observation. Exo-miR influences the migratory rate of 4T1 cells, as determined by the percentage of wound closure (Figure 4). The transfection of exo-miR concentrations of 37.5 µL/1,250,000 particles exo-miR (a) resulted in a significant inhibitory effect on 4T1 cell migration.

The independent t-test statistical analysis revealed that at 12 h after transfection into 4T1 cells, all exo-miR quantities could affect 4T1 cell migration (Figure 5). However, at 24 hours the inhibitory effect of the exo-miR nanocomplex on 4T1 cell migration was only present at the highest concentration of exo-miR at 37.5 µL/1,250,000 particles exo-miR. This indicated that the functional mimic-hsa-miR-143-3p in the exo-miR formulation was more stable and was able to significantly mediate the inhibition of 4T1 cell migration with an appropriate minimum number of particles ($p < 0.01$).

3.4. Proliferation assay using Colony Formation Assay

Colony formation assay (CFA) or clonogenic assay is an *in vitro* test to determine the ability of cells to survive and form a colony. This parameter can also be used to determine the level of cell viability and proliferation. This test is simple and appropriate for determining proliferation ability since it is non-colorimetric and non-fluorescent, resulting in minimum interference. The CFA can be used to quantify adherent cell types (Rundén-Pran et al. 2022). The CFA test will provide data on a cell capacity to control proliferation over time. This metric can be used to predict cell growth and survival in a colony. This test, however,

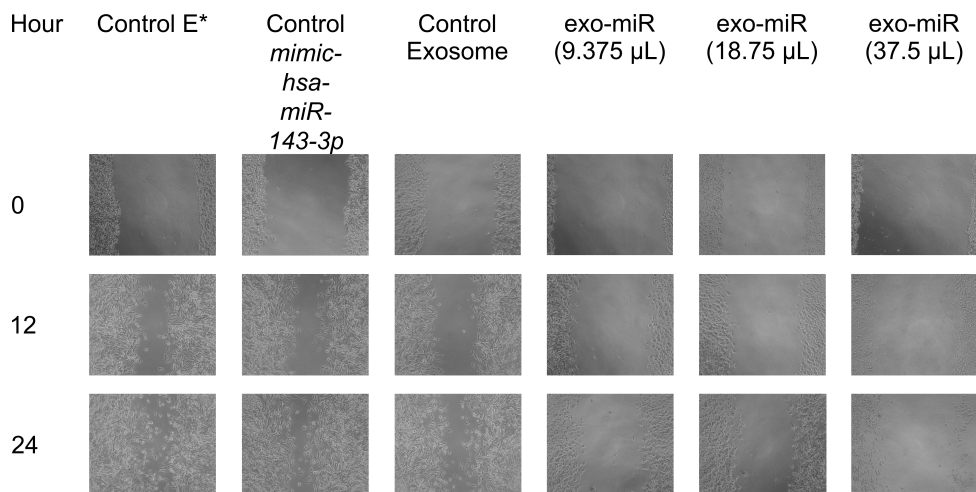


FIGURE 4 The migration of 4T1 cells was observed at 0, 12, and 24 h. Representative images from 1 of 3 replications are depicted. Cell migration was inhibited by the presence of exo-miR. The strongest inhibitory impact was observed when the concentration (a) (37.5 μL/1,250,000 particles exo-miR) of exo-miR was used for 24 h.

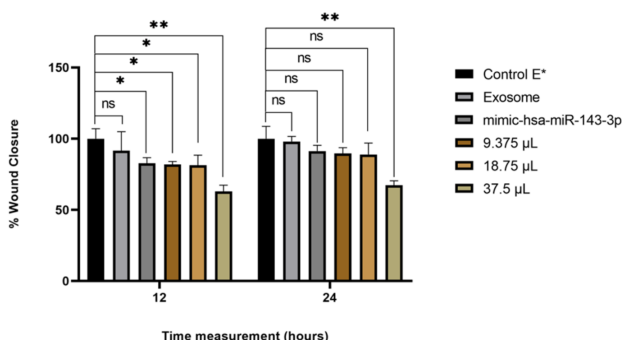


FIGURE 5 Exo-miR nanocomplex-transfected 4T1 cells showed a result on 4T1 cell migration upon wound closure. At the 12 and 24 h, the highest concentration (37.5 μL/1.250.000 particles exo-miR) had a significant effect on 4T1 cell migration compared to control. ns = not significant; * = $p < 0.05$; ** = $p < 0.01$.

cannot be used to establish whether cells are alive or dead since certain cells that are alive but not growing typically have a biological role.

The CFA test was performed by culturing cells for 10 days and adding exo-miR (150 μL/5,000,000 exo-miR, mentioned in kit’s protocol) each 72 h. The CFA was stained using methylene blue. Methylene blue staining proceeds for at least 3 hours, which corresponds to the capacity of the maximal saturation process to occur at that

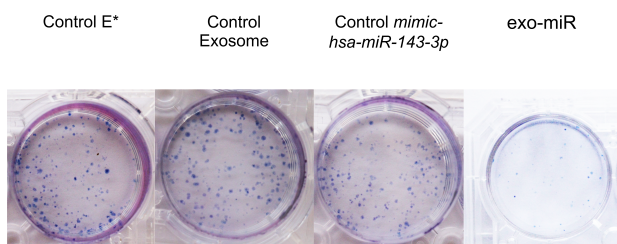


FIGURE 6 Methylene blue staining results in the colony formation assay. Representative images from 1 of 3 replications are depicted. The exo-miR nanocomplexes inhibited the growth of 4T1 cells.

time (Felice et al. 2009). The staining results were then analysed using a microscope and optiLab to generate pictures (Figure 6). ImageJ was used to count the number of colonies.

The exo-miR nanocomplex effect significantly suppressed 4T1 cell proliferation ($p < 0.001$) (Figure 7). The mimic-hsa-miR-143-3p control and the exosome control did not show any proliferation suppression effect. These data indicate that exo-miR has regulation to suppress cell proliferation compared to the administration of exosome and mimic-hsa-miR-143-3p.

According to the Hallmarks of Cancer hypothesis, cancer regulates uncontrollable growth, also known as “sustaining proliferative signaling” (Hanahan 2022). Homeostatic principles allow normal cells to govern and release signals associated to growth and division. Cancer cells are able to change this signalling, allowing them to be con-

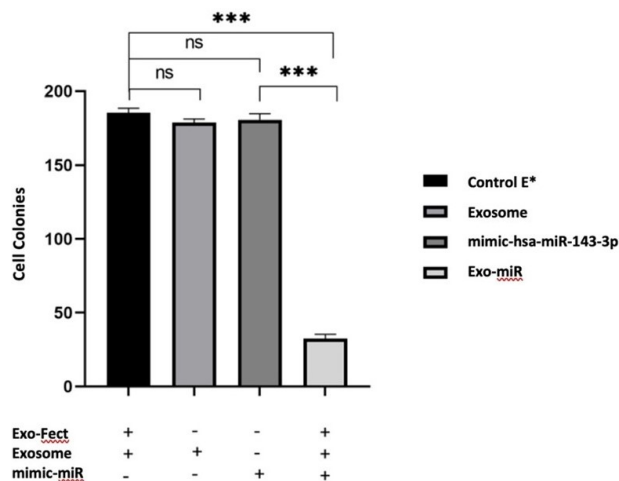


FIGURE 7 The effect of the exo-miR (150 μL/5,000,000 particle) in suppressing the proliferation of the 4T1 cell line compared to control exosomes and mimic-hsa-miR-143-3p. ns = not significant; **, $p < 0.01$.

trolled for continuously growth and proliferation. Several cancer cell strategies for controlling continuous proliferation include the synthesis of growth factor ligands, which are mediated through their receptors, modifying proliferation stimulation. miR-143-3p modulation at this epigenetic level can target genes involved in cancer cell growth.

miRNA-based therapy has shown clinical potential for cancer treatment. Additionally, Kadriyan et al. (2021) reported that exosomes from nasopharyngeal carcinoma carry both wild type and mutant P53, indicating the potency of exosome as a biomarker and/or therapy approach.

In summary, our study shows the potential of mimic-miR encapsulated exosome to suppress the viability, migration and proliferation in 4T1 cell line. The 4T1 mouse mammary tumor cell line is an animal model for stage IV human breast cancer that is highly invasive and metastasize efficiently. Although this study has shown the significant effect of exo-miR, more research is required to gather more validating data by using human breast cancer cell line and its implication in normal cells. Additionally, the molecular mechanisms and signaling pathway of exo-miR in tumor microenvironment are warranted for further investigation.

4. Conclusions

The exosome has a 177 nm diameter, a particle concentration of 2.4×10^8 particles/mL, and a spherical particle shape. The concentrations of exo-miR 7.5 μ L/ 250,000 particles exo-miR significantly affected for 4T1 cell viability ($P < 0.001$) by up to 58% compared to the control (99.7%). The Wound Closure percentage of 67% at 24 hours suggested that an exo-miR at concentrations of 37.5 μ L/ 1,250,000 particles exo-miR significantly inhibit the migratory rate of 4T1 cells ($P < 0.01$). Exo-miR volume of 150 μ L (5,000,000 particles exo-miR) significantly inhibit 4T1 cell proliferation and ability to form colonies ($P < 0.001$), as seen by the low number of colonies (32 colonies) compared to controls (185 colonies). This finding showed that the miR-mimic nanocomplex and exosomes have the potential to be applied as targeted therapies in cancer cases. Moreover, the exosomes must be studied and identified beforehand to ensure that the endogenous components of exosomes are not interfering in target cells.

Acknowledgments

The research was funded by Center for Higher Education Funding (BPPT) and Indonesia Endowment Fund for Education (LPDP).

Authors' contributions

SMH, DAAN, PBS designed the study. FN carried out the laboratory work, analyzed the data and wrote the manuscript. All authors read and approved the final version of the manuscript.

Competing interests

The authors declare no conflicts of interest.

References

- Agung Nugrahaningsih DA, Purwadi P, Sarifin I, Bachtiar I, Sunarto S, Ubaidillah U, Larasati I, Satriyo PB, Setiasari DW, Hasanah MN, At-thobari J, Mubarika S. 2023. In vivo immunomodulatory effect and safety of MSC-derived secretome. *F1000Research* 12:421. doi:10.12688/f1000research.131487.1.
- Bhorne R, Del Vecchio F, Lee GH, Bullock MD, Primrose JN, Sayan AE, Mirnezami AH. 2018. Exosomal microRNAs (exomiRs): Small molecules with a big role in cancer. *Cancer Lett.* 420:228–235. doi:10.1016/j.canlet.2018.02.002.
- Dasgupta I, Chatterjee A. 2021. Recent advances in miRNA delivery systems. *Methods Protoc.* 4(1):10. doi:10.3390/mps4010010.
- de Abreu RC, Ramos CV, Becher C, Lino M, Jesus C, da Costa Martins PA, Martins PA, Moreno MJ, Fernandes H, Ferreira L. 2021. Exogenous loading of miRNAs into small extracellular vesicles. *J. Extracell. Vesicles* 10(10):e12111. doi:10.1002/jev2.12111.
- Felice DL, Sun J, Liu RH. 2009. A modified methylene blue assay for accurate cell counting. *J. Funct. Foods* 1(1):109–118. doi:10.1016/j.jff.2008.09.014.
- Global Cancer Observatory. 2020. Global Cancer Observatory 2020. Lyon: International Agency for Research on Cancer (IARC). URL <https://gco.iarc.fr/en>.
- Guo M, Li R, Yang L, Zhu Q, Han M, Chen Z, Ruan F, Yuan Y, Liu Z, Huang B, Bai M, Wang H, Zhang C, Tang C. 2021. Evaluation of exosomal miRNAs as potential diagnostic biomarkers for acute myocardial infarction using next-generation sequencing. *Ann. Transl. Med.* 9(3):219. doi:10.21037/atm-20-2337.
- Hanahan D. 2022. Hallmarks of cancer: New dimensions. *Cancer Discov.* 12(1):31–46. doi:10.1158/2159-8290.CD-21-1059.
- Hermansyah D, Rahayu Y, Azrah A, Pricilia G, Sufida S, Rifsal D, Simarmata A. 2021. Triple-negative breast cancer clinicopathology: A single-center experience. *Indones. J. Cancer* 15(3):125–128. doi:10.33371/ijoc.v15i3.791.
- Heusermann W, Hean J, Trojer D, Steib E, von Bueren S, Graff-Meyer A, Genoud C, Martin K, Pizzato N, Voshol J, Morrissey DV, Andaloussi SE, Wood MJ, Meisner-Kober NC. 2016. Exosomes surf on filopodia to enter cells at endocytic hot spots, traffic within endosomes, and are targeted to the ER. *J. Cell Biol.* 213(2):173–184. doi:10.1083/jcb.201506084.
- Jonkman JE, Cathcart JA, Xu F, Bartolini ME, Amon JE, Stevens KM, Colarusso P. 2014. An introduction to the wound healing assay using live-cell microscopy. *Cell Adhes. Migr.* 8(5):440–451. doi:10.4161/cam.36224.

- Kadriyan H, Prasedya ES, Pieter NAL, Gaffar M, Akil A, Bukhari A, Budu B, Zainuddin AA, Masadah R, Rhomdoni AC, Punagi AQ. 2021. NPC-exosome carry wild and mutant-type p53 among nasopharyngeal cancer patients. *Indones. Biomed. J.* 13(4):403–408. doi:10.18585/INABJ.V13I4.1718.
- Kim H, Jang H, Cho H, Choi J, Hwang KY, Choi Y, Kim SH, Yang Y. 2021. Recent advances in exosome based drug delivery for cancer therapy. *Cancers (Basel)*. 13(17):4435. doi:10.3390/cancers13174435.
- Klinge CM. 2018. Non-coding RNAs in breast cancer: Intracellular and intercellular communication. *Non-coding RNA* 4(4):40. doi:10.3390/ncrna4040040.
- Lu ZG, Shen J, Yang J, Wang JW, Zhao RC, Zhang TL, Guo J, Zhang X. 2023. Nucleic acid drug vectors for diagnosis and treatment of brain diseases. *Signal Transduct. Target. Ther.* 8:39. doi:10.1038/s41392-022-01298-z.
- Mehanna J, Haddad FG, Eid R, Lambertini M, Kourie HR. 2019. Triple-negative breast cancer: Current perspective on the evolving therapeutic landscape. *Int. J. Womens. Health* 11:431–437. doi:10.2147/IJWH.S178349.
- Radosa JC, Eaton A, Stempel M, Khandar A, Liedtke C, Solomayer EF, Karsten M, Pilewskie M, Morrow M, King TA. 2017. Evaluation of local and distant recurrence patterns in patients with triple-negative breast cancer according to age. *Ann. Surg. Oncol.* 24(3):698–704. doi:10.1245/s10434-016-5631-3.
- Rayson D, Payne JJ, Michael JC, Tsuruda KM, Abdollell M, Barnes PJ. 2018. Impact of detection method and age on survival outcomes in triple-negative breast cancer: A population-based cohort analysis. *Clin. Breast Cancer* 18(5):e955–e960. doi:10.1016/j.clbc.2018.04.013.
- Rundén-Pran E, Mariussen E, El Yamani N, Elje E, Longhin EM, Dusinska M. 2022. The colony forming efficiency assay for toxicity testing of nanomaterials—Modifications for higher-throughput. *Front. Toxicol.* 4:983316. doi:10.3389/ftox.2022.983316.
- Samanta S, Rajasingh S, Drosos N, Zhou Z, Dawn B, Rajasingh J. 2018. Exosomes: New molecular targets of diseases. *Acta Pharmacol. Sin.* 39(4):501–513. doi:10.1038/aps.2017.162.
- Satriyo P, Yeh CT, Chen JH, Aryandono T, Haryana S, Chao TY. 2020. Dual therapeutic strategy targeting tumor cells and tumor microenvironment in triple-negative breast cancer. *J. Cancer Res. Pract.* 7(4):139–148. doi:10.4103/jcrp.jcrp_13_20.
- Stockert JC, Horobin RW, Colombo LL, Blázquez-Castro A. 2018. Tetrazolium salts and formazan products in Cell Biology: Viability assessment, fluorescence imaging, and labeling perspectives. *Acta Histochem.* 120(3):159–167. doi:10.1016/j.acthis.2018.02.005.
- Vallabhaneni KC, Penfornis P, Dhule S, Guillonneau F, Adams KV, Yuan Mo Y, Xu R, Liu Y, Watabe K, Vemuri MC, Pochampally R. 2014. Extracellular vesicles from bone marrow mesenchymal stem/ stromal cells transport tumor regulatory microRNA, proteins, and metabolites. *Oncotarget* 6:4953–4967.
- Vestad B, Llorente A, Neurauter A, Phuyal S, Kierulf B, Kierulf P, Skotland T, Sandvig K, Haug KBF, Øvstebø R. 2017. Size and concentration analyses of extracellular vesicles by nanoparticle tracking analysis: a variation study. *J. Extracell. Vesicles* 6(1):1344087. doi:10.1080/20013078.2017.1344087.
- Wang S, Lu J, You Q, Huang H, Chen Y, Liu K. 2016. The mTOR/AP-1/VEGF signaling pathway regulates vascular endothelial cell growth. *Oncotarget* 7(33):53269–53276. doi:10.18632/oncotarget.10756.
- Xia C, Yang Y, Kong F, Kong Q, Shan C. 2018. MiR-143-3p inhibits the proliferation, cell migration and invasion of human breast cancer cells by modulating the expression of MAPK7. *Biochimie* 147:98–104. doi:10.1016/j.biochi.2018.01.003.
- Ysrafil Y, Astuti I, Anwar SL, Martien R, Sumadi FAN, Wardhana T, Haryana SM. 2020. MicroRNA-155-5p diminishes *in vitro* ovarian cancer cell viability by targeting HIF1 α expression. *Adv. Pharm. Bull.* 10(4):630–637. doi:10.34172/apb.2020.076.
- Zhang D, Lee H, Zhu Z, Minhas JK, Jin Y. 2016. Enrichment of selective miRNAs in exosomes and delivery of exosomal miRNAs *in vitro* and *in vivo*. *Am. J. Physiol. - Lung Cell. Mol. Physiol.* 312(1):L110–L121. doi:10.1152/ajplung.00423.2016.